

Supplementary information

CIP2A mediates mitotic recruitment of SLX4/MUS81/XPF to replication stress-induced DNA lesions to maintain genome integrity

Lauren de Haan, Sietse J. Dijt, Alejandro García-López, Dan Ruan, Panagiotis Martzios, Femke J. Bakker, Marieke Everts, Harry Warner, Frank N. Mol, J. Ross Chapman, H. Rudolf de Boer, Bert van de Kooij, Pim J. Huis in 't Veld, Rifka Vlijm, Marcel A.T.M. van Vugt.

This file includes:

Supplementary methods

Supplementary Figure 1

Supplementary Figure 2

Supplementary Figure 3

Supplementary Figure 4

Supplementary Figure 5

Supplementary Figure 6

Supplementary Figure 7

Supplementary Figure 8

Supplementary Figure 9

Supplementary Figure 10

Supplementary Methods

Viral transductions

To establish CIP2A reconstituted RPE1 *TP53*^{-/-}, HEK293T cells were transfected with indicated pMSCV plasmids in combination of pRetro-VSV-G, pRetro-gag/pol and pAdvantage. Virus containing supernatant was harvested 48 h after transfection and filtered a 0.45 µm syringe filter. Virus-containing supernatant with 4 µg/mL of polybrene was subsequently used to infect target cells for 12 h. Transduced reconstituted cell lines were selected with 10 µg/mL blasticidin.

To generate doxycycline-inducible shRNA expressing cell lines, cells were transduced with indicated lentiviral pLKO shRNA plasmids. In brief, HEK293T cells were transfected with Tet-pLKO-puro vector with indicated shRNAs in combination with the lentiviral packaging plasmids pMD2.G and psPAX2. Virus containing supernatant was harvested 48 h and 56 h after transfection and filtered through a 0.45 µm syringe filter. Virus-containing supernatant with 4 µg/mL of polybrene was subsequently used to infect the target cells for 12 h. RPE1 *TP53*^{-/-}, RPE1 *TP53*^{-/-} *CIP2A*^{-/-} and *TP53*^{-/-} *CIP2A*^{-/-} cells expressing CIP2A mutants were transduced with indicated pLKO shRNAs and were selected with 15 µg/mL puromycin. BT549 cells transduced with pLKO shRNAs were selected with 1 µg/mL puromycin. Cells were harvested for Western blot, seeded for clonogenic survival assays, or fixed for immunofluorescence 48 h after shRNA induction by addition of 1 µg/mL doxycycline.

Immunofluorescence microscopy

Cells were seeded on glass coverslips in 6-well or 12-well plates at 48 h prior to treatments. If indicated, cells were treated for 16 h with low dose APH (200 nM, Merck) before addition of RO-3306 (5 µM, Axon Medchem) for 4 h to arrest cells at G2/M-border. RO-3306 was washed out from synchronized cells to allow entry into mitosis by washing once with pre-warmed PBS, followed by releasing the cells in complete medium. For analysis of IR-induced DNA damage foci in mitosis, cells were irradiated with 0.25 Gy 5 min after release using a Cesium¹³⁷ source and fixed 30 min after release. For micronuclei quantification, asynchronous cells were treated for 24 h with 200 nM APH before fixation or cells were treated with 3 Gy IR and recovered for 72 h before fixation. For MiDAS analysis, 20 µM EdU was added to complete medium during

release. For ATM and ATR inhibition cells were pretreated 30 min before RO-3306 release with either 10 μ M ATRi KU55933 (Axon Medchem) or 10 μ M ATMi VE-821 (MedChem Express), and subsequently released in presence of the inhibitors. Cells were fixed 25 min after release for 15 min using 2% paraformaldehyde in PBS. After fixation, cells were permeabilized with 0.5% Triton-X in PBS for 10 min. For MiDAS, EdU Click-IT reaction was performed for 30 min at room temperature according to protocol Click-IT™ EdU Cell Proliferation Kit for Imaging (Invitrogen). Cells were subsequently incubated for 1 h with blocking buffer containing 2% bovine serum albumin (BSA) and 0.05% Tween in PBS (PBT). Incubation with primary antibodies was performed overnight at 4° Celsius with indicated antibodies in PBT. The following antibodies were used: mouse anti- γ H2AX (Millipore, 05-636, 1:400), rabbit anti- γ H2AX (Cell Signaling, 9718, 1:400), mouse anti-CIP2A (Santa Cruz, sc-80659, 1:500), rabbit anti-CIP2A (Invitrogen, PA5-83469, 1:300), rabbit anti-TOPBP1 (Bethyl, A300-111A-M, 1:400), mouse anti-ERCC1 (Santa Cruz, sc-17809, 1:100), rabbit anti-XPF (Abcam, ab76948, 1:100), mouse anti-MUS81 (Abcam, ab14387, 1:100), mouse anti-BTBD12 (SLX4) (Abnova, H000844644-B01P, 1:500), mouse anti-V5 (Invitrogen, R960-25, 1:400), rabbit anti-V5 (Cell signaling, 13202S, 1:1000), rabbit anti-RAD52 (Abcam, ab124971, 1:300). After washing the coverslips to remove residual primary antibodies, incubation with DAPI and the following secondary antibodies: 488 goat anti-mouse (Thermofisher, A11029, 1:500), 488 goat anti-rabbit (Thermofisher, A11008, 1:500), 488 donkey anti-rabbit (Thermofisher, A21206, 1:500), 647 goat anti-mouse (Thermofisher, A32728, 1:500), 647 donkey anti-rabbit (Thermofisher, A31573, 1:500), 647 donkey anti-mouse (1:500) in PBT was performed at room temperature. For micronuclei analysis, cells were only incubated with DAPI after permeabilization. Coverslips were extensively washed and subsequently mounted with Prolong Gold antifade reagents (Life Technologies). Images were acquired using Zeiss Axio Imager 2 using a 40x or 63x objective with the Zen 3.0 software (Zeiss) or on a Leica DM6000B microscope using a 10x or 40x objective with LAS-AF software (Leica), and analysis was performed using FIJI (ImageJ). Numbers of foci as well as co-localization were manually quantified using FIJI software, based on maximal image projections of multiple Z-stack (0.1 μ m each). V5 and TOPBP1 foci intensity were quantified using the ImageJ macro 'Foci-analyzer' (freely available at <https://github.com/Biolmaging-NKI/Foci-analyzer>; created by Bram van den Broek, the Netherlands Cancer Institute, the Netherlands). Fluorescence signal intensities are depicted as arbitrary units, and

are normalized by dividing the mean foci intensity per cell by the median intensity of RPE1 *TP53*^{-/-} *CIP2A*^{-/-} cells with reconstituted CIP2A-WT-V5 per individual experiment.

For Airyscan analysis, RPE1 *TP53*^{-/-} cells were seeded on glass coverslips, with APH (200 nM). After 4 h, the medium was replaced with medium containing 7.5 μ M RO-3306 and 200 nM APH for an additional 16 h. RO-3306 was washed away with three PBS washes and three washes with medium. Cells were fixed after 1 h with 4% paraformaldehyde in PBS (20 min) and permeabilized with 0.5% Triton X-100 in PBS (10 min) at room temperature. Primary antibodies mouse anti-PICH (Abnova H00054821-B01P) was used at 1:500 for 1.5 h at 37°C, rabbit anti-CIP2A (Invitrogen PA5-83469) was used at 1:300 for 2 h at room temperature. Donkey anti-rabbit AF488 (Invitrogen A32790) and donkey anti-mouse AF555 (Invitrogen A31570) secondary antibodies were used at 1:1000 for 1h at room temperature as follows. Coverslips were mounted with medium containing DAPI (Invitrogen P36962). Images were acquired with a Zeiss LSM 980 microscope equipped with Airyscan 2 and a Plan-Apochromat 63 \times /1.4 Oil DIC M27 objective (WD 0.19 mm). Z-stacks were collected at 120 nm intervals, processed with Airyscan in ZEN Blue software and analyzed with Fiji.

STED microscopy

For STED microscopy, cells were seeded, treated and fixed similar as described above for immunofluorescence microscopy, with the following exception: cells were fixed 30 min after RO-3306 washout to obtain cells at early mitotic stages, whereas cells were fixed at 60 min and 90 min after RO-3306 washout to obtain cells at later stages of mitosis. STED microscopy slide preparation was performed largely as previously described for fixed HEK293T cells⁶⁸. Specifically, cells were incubated with 2% BSA, 10% goat serum, and 0.05% Tween as blocking buffer. This specific blocking buffer was used for both primary and secondary antibody incubations. Primary antibodies were used as earlier described, and the following secondary antibodies were used: 580 goat anti-mouse (Abberior STAR, ST580-1001, 1:80), 580 goat anti-rabbit (Abberior STAR, ST580-1002, 1:80), 635 goat-anti mouse (Abberior STAR, ST635-1001, 1:80), 635 goat anti-rabbit (Abberior STAR, ST635-1002, 1:80), 488 donkey anti-rabbit (Thermofisher, A21206, 1:500).

STED imaging of fixed samples was performed on a STED microscope (Abberior Expert Line) with a 100× oil immersion objective (Olympus Objective UPlanSApo 100×/1.40 oil). Laser alignments were optimized before imaging using a 0.1-μm bead sample (Invitrogen, TetraSpeck T7279). During imaging, z-stacks of cells were made at confocal resolution and all CIP2A foci in each cell were subsequently selected manually and individually imaged at STED resolution using a custom Python script adapted from Mol and Vlijm⁶⁹. All STED images were acquired with a pixel size of 22 nm (unless specified otherwise), a pixel dwell time of 20 μs and a 0.6 Airy Units (AU) pinhole, with image size varying based on structure size. For excitation, we used 40 MHz pulsed lasers with a wavelength of 561 nm (203 μW at laser head) and 640 nm (1 mW at laser head) and a continuous wave laser with a wavelength of 405 nm for DAPI excitation (confocal only). A 40 MHz pulsed laser (3.0 W) with a wavelength of 775 nm was used for depletion. Detection filters were set to 699 ± 52 nm for the 640 channel (640 nm excitation), 600 ± 31 nm for the 561 channel (561 nm excitation) and 525 ± 27 nm for the 488 channel (488 nm excitation). The 640 and 561 channel were collected separately per line, except for EdU-CIP2A images, in which both channels were collected in separate images (first 640 nm then 561 nm channel) to prevent bleaching of the Alexa Fluor 647 dye during imaging of the 561 nm channel. For EdU-CIP2A-γH2AX images, all channels were collected in separate images (first 488 nm, then 640 nm, and finally 561 nm channel). The applied laser powers, dwell times, line steps and gating for STED imaging were optimized for the different samples and dyes: STAR 635 (0.9-1.5% excitation (640 nm), 28-35% STED, 12-24 lines, 0.75-1.2 ns gating delay, 9.0 ns gating width), STAR 580 (4.1-25.0% excitation (561 nm), 45-60% STED, 12 lines, 0.45-1.0 ns gating delay, 9.0 ns gating width). For EdU-CIP2A samples, the following settings were used: EdU/Alexa Fluor™ 647 (1.9-2.0% excitation (640 nm), 4% STED, 6 lines, gating off), CIP2A/STAR 580 (17.2-50.0% excitation (561 nm), 50% STED, 12 lines, gating off). For EdU-CIP2A-γH2AX samples, the following settings were used: EdU/Alexa Fluor™ 647 (44 nm pixels, 2.0% excitation (640 nm), 3% STED, 12 lines, 0.75 ns gating delay, 9.0 ns gating width), CIP2A/STAR 580 (22 nm pixels, 35% excitation (561 nm), 50% STED, 12 lines, 0.75 ns gating delay, 9.0 ns gating width), γH2AX/Alexa Fluor™ 488 (66 nm pixels, 2% excitation (488 nm), confocal, 3 lines, gating off).

STED image processing

All STED images shown in the figures were deconvoluted using a custom-written Wiener filter (Mol, F. N., & Vlijm, R. (2025). Interactive Wiener Filter (v1.0), and can be found on Zenodo: <https://doi.org/10.5281/zenodo.15075206>), All raw STED images can be found on DataverseNL (<https://doi.org/10.34894/O3KAFO>). Deconvolution parameters were optimized manually per image to get background subtraction of 2-50 counts (640 channel) or 2-30 counts (561 channel), STED/confocal ratio of 0.70.9 (640 channel) or 0.6-0.8 (561 channel), noise-to-signal ratio of 0.050.3 (640 channel) or 0.060.25 (561 channel) and point-spread functions of 26-35 nm (STED) and 350 nm (confocal) for the 640 channel or 30-35 nm (STED) and 300 nm (confocal) for the 561 channel. For EdU in EdU-CIP2A- γ H2AX images, a 50 nm STED point-spread function was used. To merge EdU-CIP2A- γ H2AX images, EdU and γ H2AX images were rescaled to 22 nm pixels with no interpolation. Due to the large spread in intensities, linear intensity scaling was applied separately for each image. The structure length was determined by multiplying the manually measured length in pixels by the pixel size of 22 nm. These structure size measurements were performed using FIJI (ImageJ). Line profiles were drawn in FIJI with a line width of 3 pixels and a segmented line with spline fit was used for curved line profiles. CIP2A structures were manually classified. Loop-containing structures were defined by having a continuous ring-like structure, with absence of labeling in the inner core. Filamentous structures were based on their line-like appearance. Remaining structures were classified as unstructured, and no obvious other categories were observed. The numbers of CIP2A-TOPBP1 structures per telophase in Fig. 1f and 1g may be an overestimation of the actual number, as only cells with CIP2A-TOPBP1 structures were measured. Structure size in Fig. 1i was determined by measuring the length of the longest axis by drawing a line through the entire structure as shown in Supplemental Fig. 2c. Elongation measurements in Supplementary Figure 2d were performed by dividing the length of the longest axis by the length of the shortest axis for each loop-containing structure. For Figure 5j-l, we additionally included 'loop-like' and 'filament-like' for cells expressing CIP2A Δ C. In these experiments, signal that appeared in a ring-like shape, but was not continuous was labeled as 'loop-like'. Similarly, CIP2A staining that resembled line-like appearances, but was not continuous was labeled as 'filament-like'. The elongation of

loop-containing CIP2A structures was analyzed by dividing the length of longest axis by the length of shortest axis.

Co-immunoprecipitation

RPE1 *TP53*^{-/-} and RPE1 *TP53*^{-/-} *CIP2A*^{-/-} cl#1 cells were seeded in T175 flasks for co-immunoprecipitation (IP) of endogenous CIP2A in mitotic cells. For IP in irradiated conditions, cells were treated with 62.5 ng/mL nocodazole for 16 h prior to mitotic shake off to harvest mitotic cells. Mitotic cells were either left untreated (control) or treated with 5 Gy irradiation and recovered for 1 h before adding ice-cold MPER lysis buffer (Thermofisher), complemented with protease and phosphatase inhibitor cocktail (Thermofisher) and 5 units/mL benzonase (Santa Cruz) ('complete lysis buffer'). For IP in APH-treated cells, cells were either left untreated (control) or treated with 200 nM APH for 16 h prior to adding 5 μ M RO-3306 for 4 h. APH treated cells were subsequently pre-treated 30 min before release with 5 mM hydroxyurea (HU). Synchronized cells were released from RO-3306 by washing once with pre-heated PBS, followed by RO-3306 wash-out using complete medium including 62.5 ng/mL nocodazole (control) or 62.5 ng/mL nocodazole and 5 mM HU (APH treated cells) to accumulate cells in mitosis. Mitotic shake off was performed at 1 h after release and cells were lysed with ice-cold complete lysis buffer.

Both APH and IR samples were tumbled end-over-end for 30 min at 4° Celsius after addition of complete lysis buffer, and subsequently centrifuged for 15 min at 12,000 rpm to clear whole cell lysates. The protein concentration of the supernatant was quantified using Pierce BCA Protein Assay Kit (Thermofisher). 1 μ g of CIP2A antibody was added to the pre-cleared whole cell lysates for 1 h and tumbled end-over-end at 4 degrees Celsius. Subsequently, magnetic Dynabeads Protein G beads (Thermofisher) for immunoprecipitation were added to the lysates and incubated for another hour at 4° Celsius. Beads were precipitated using a magnet and were washed 3 times with low salt buffer (20 mM HEPES pH 7.5, 150 M NaCl in dH₂O), and a final wash with high salt buffer (20 mM HEPES pH 7.5, 496 M NaCl in dH₂O). Protein samples for western blot analysis were eluted from the beads after this final high salt wash step by boiling the beads in 2x SDS-sample buffer with beta-mercaptoethanol, whereas samples for mass spectrometry were dissolved in denaturing buffer (8M Urea 100 mM Tris pH8.0) and snap frozen.

Mass spectrometry

Eight biological samples were subjected to on-bead digestion of immunoprecipitated proteins, bead mixtures were subjected to cysteine reduction (1.5 mM dithiothreitol for 15 min at 30°C), followed by alkylation (7.5 mM iodoacetamide, 30 min at RT). Bead mixture was diluted to 2M Urea with 100 mM ammonium bicarbonate and digested with 100 ng trypsin (Promega) overnight at 37°C. After bead removal, peptides were acidified with 0.1% formic acid, extracted by solid phase extraction with C18 cartridges (Gracepure SPE C18-Aq), and dried by SpeedVac (Thermofischer). Lastly, extracted peptides were resuspended in 0.1% formic acid. Discovery mass spectrometric analyses were performed on a quadrupole orbitrap mass spectrometer equipped with a nano-electrospray ion source (Orbitrap Exploris 480, Thermo Scientific). Chromatographic separation of the peptides was performed by liquid chromatography (LC) on a Evosep system (Evosep One, Evosep) using a nano-LC column (EV1137 Performance column 15 cm x 150 µm, 1.5 µm, Evosep; buffer A: 0.1% v/v formic acid, dissolved in milliQ-H₂O, buffer B: 0.1% v/v formic acid, dissolved in acetonitrile). Twenty µL of the diluted digests were injected in triplicate and separated using the 30SPD workflow (Evosep). The mass spectrometer was operated in positive ion mode and data-independent acquisition mode (DIA) using isolation windows of 16 m/z with a precursor mass range of 400-1000, switching the FAIMS between CV-45V and -60V with three scheduled MS1 scans during each screening of the precursor mass range. Acquired spectra were analyzed using Spectronaut v18.1.230626 (Biognosys) with the standard settings of the directDIA workflow except that quantification was performed on MS1 with a human SwissProt database (www.uniprot.org, UP000005640 release 2023_1, 20422 entries). For the quantification, the Q-value filtering was set to the classic setting with global normalization and no imputation.

Normalized intensity values were processed using Perseus v1.6.15 (MaxQuant). Data was log₂ transformed, after which the three technical replicate measurements per sample were grouped and filtered to keep each protein with three valid values in at least one group. Lastly, missing data was imputed with random values obtained from a gaussian distribution with a downshift of 1.8x standard deviation of each sample and a width of 0.3x the standard deviation. Experimental differences and statistical analyses were obtained in Perseus using the Volcano plot function, which uses a Significance Analysis of Microarrays test (two-sided t-test, 250 randomizations, FDR=0.05 and S0=0.1). The mass spectrometry proteomics data have been deposited

to the ProteomeXchange Consortium via the PRIDE partner repository with the dataset identifier PXD059881 (<https://www.ebi.ac.uk/pride/archive/projects/PXD059881>).

Western blot

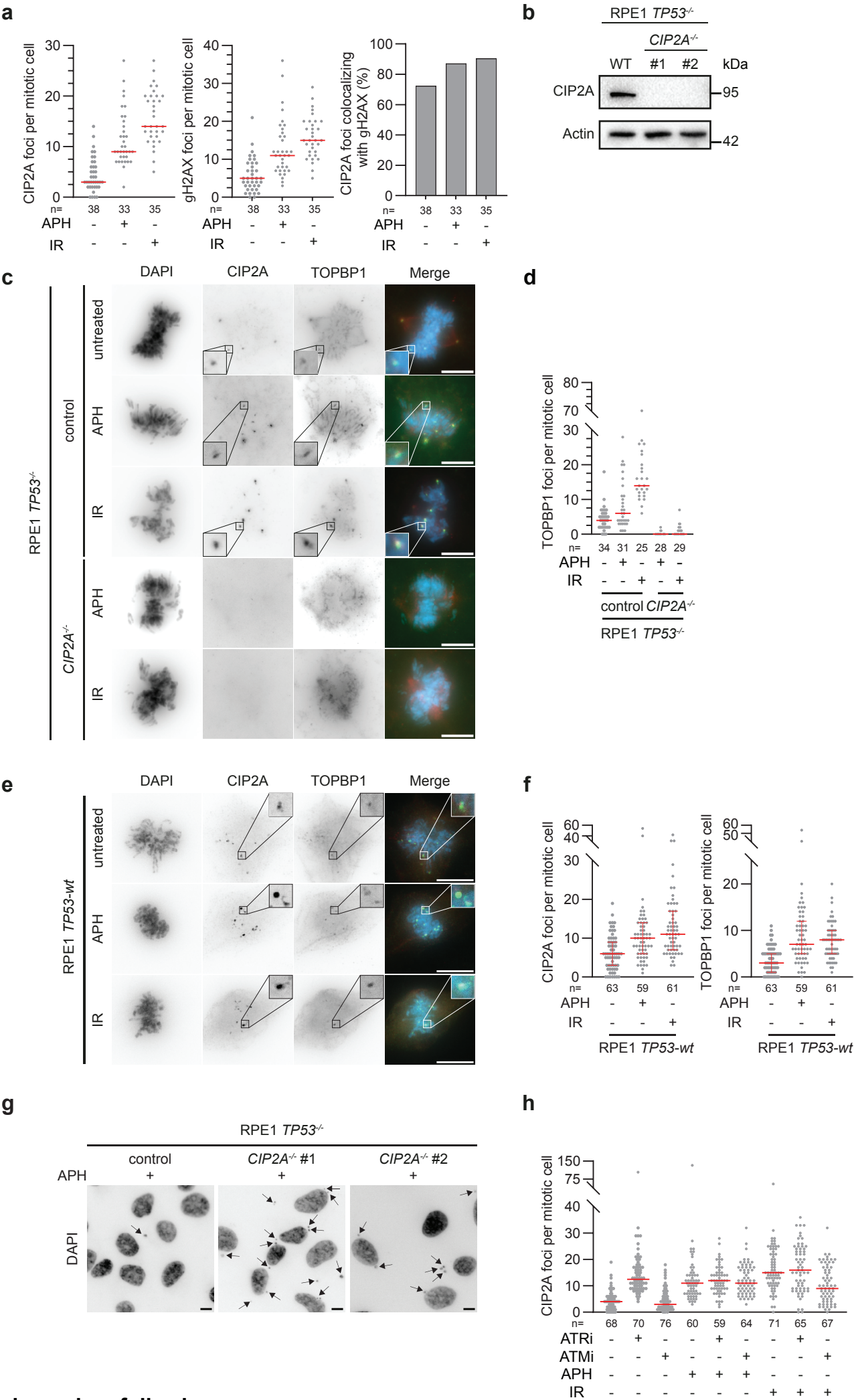
Cells were lysed with MPER lysis buffer (ThermoFisher), complemented with protease and phosphatase inhibitor cocktail (ThermoFisher) in presence or absence of benzonase (100 units/mL, Merck) and EDTA (5 mM, ThermoFisher). Protein concentration was measured using the PierceTM BCA Protein Assay Kit (ThermoFisher). Proteins were subsequently separated using SDS-polyacrylamide gels, and transferred to PVDF membrane (conventional transfer: Immobilon, turbo transfer: Bio-Rad). Membranes were blocked with 5% skimmed milk (Sigma) in Tris-buffered saline (TBS) with 0,05% Tween (TBS-T) or 3% BSA (Sigma) in TBS-T. Membranes were incubated with the following antibodies: mouse anti-CIP2A (Santa Cruz, sc-80659, 1:500), rabbit anti-TOPBP1 (Bethyl, A300-111A-M, 1:1000), rabbit anti- γ H2AX (Cell signaling, 9718, 1:1000), mouse anti-Actin (MP Biomedicals, 69100, 1:10.000), HRP conjugated Beta-Actin (Proteintech, HRP-60008, 1:10.000), rabbit anti-GAPDH (Abcam, ab128915, 1:1000), rabbit anti-MDC1 (Abcam, ab11171, 1:1000), mouse anti-MUS81 (Abcam, ab14387, 1:1000), rabbit anti-Vinculin (Abcam, ab129002, 1:5.000), mouse anti-BTBD12 (SLX4) (Abnova, H00084464-B01P, 1:1000), mouse anti-BRCA1 (Sigma-Aldrich, OP92, 1:250), rabbit anti-XPF (Abcam, ab76948, 1:1000), mouse anti-BRCA2 (Calbiochem, OP95, 1:1000), mouse anti-HSP90 α/β (F-8) (Santa Cruz, sc-13119, 1:10.000), rabbit α -tubulin (Cell signaling, 2125, 1:1000) overnight at 4° Celsius. Membranes were extensively washed and incubated with the following horse-radish peroxidase-conjugated secondary antibodies: HRP-conjugated rabbit anti-mouse (DAKO, 1:5000) and HRP-conjugated goat anti-rabbit (DAKO, 1:5000) for 1 h at room temperature and visualized using Lumi-light or SuperSignal West Femto Maximum Sensitivity Substrate (ThermoFisher). Images were acquired with a ChemiDoc MP imaging system (Bio-Rad).

Clonogenic survival assays

RPE1 cells with either shLUC or shBRCA2 were pretreated for 48h with 1 μ g/mL doxycycline before seeding 100 or 200 into a 6-well plate. Fresh doxycycline was added during seeding, and medium was not refreshed during the entire experiment.

Cells were fixed with methanol and stained with staining buffer (50% methanol, 29,95% water, 20% acetic acid and 0.05% Coomassie Brilliant Blue) 7-9 days after seeding. Colonies were imaged using an EliSpot reader (Alpha Diagnostics International) with vSpot Spectrum software. The number of colonies were manually counted.

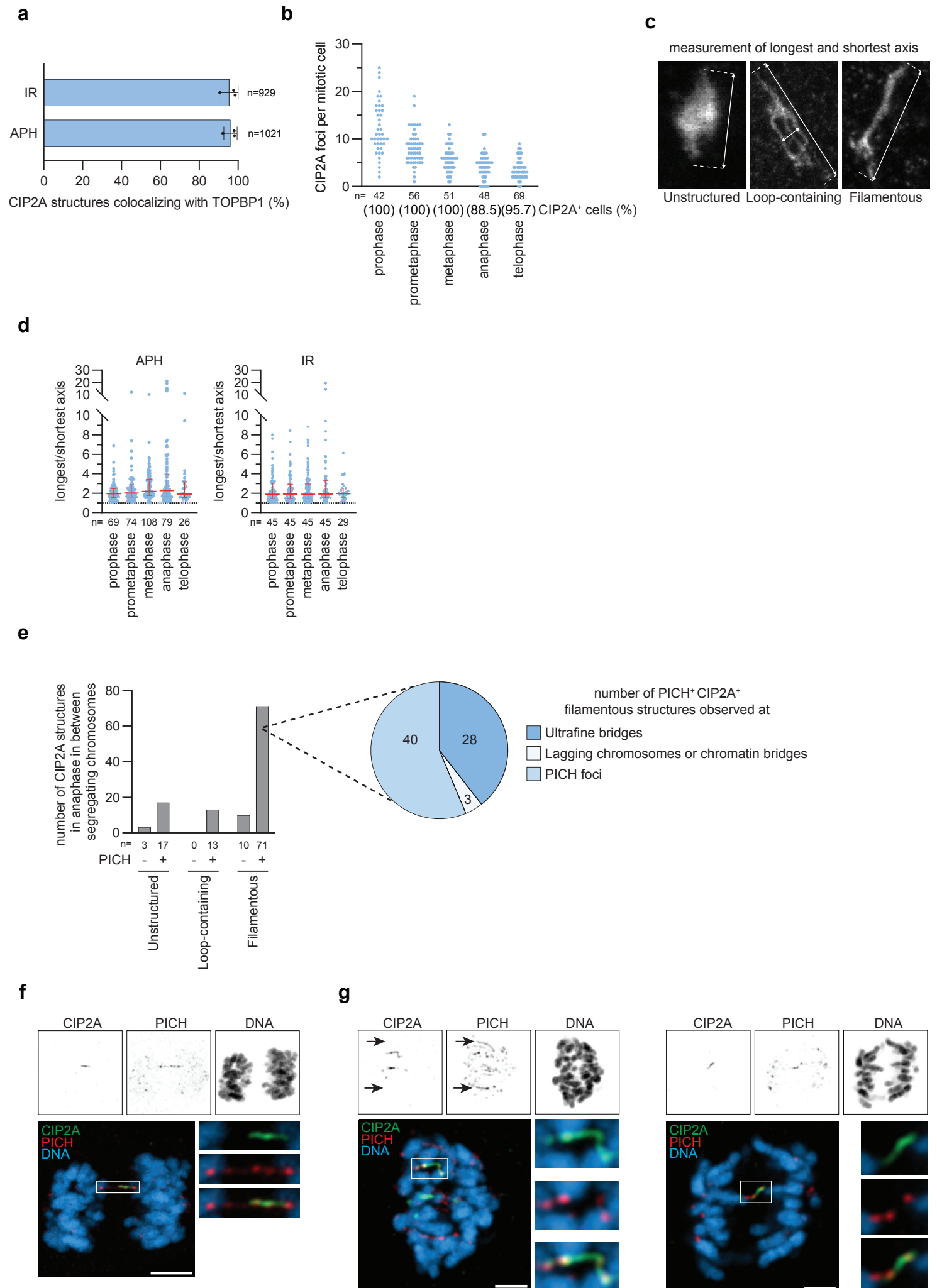
Supplemental Figure 1



Supplemental Figure 1: Different types of mitotic DNA damage recruit CIP2A-TOPBP1

(a) Quantification of CIP2A foci colocalizing with γ H2AX foci in RPE1 *TP53*^{-/-} cells, untreated or after treatment with APH (200 nM, 20 h) or IR (0,25 Gy). Data from one experiment are shown. **(b)** Western blot analysis of CIP2A in parental RPE1 *TP53*^{-/-} cells or *CIP2A*^{-/-} clones. Lysates were immunoblotted for indicated proteins. **(c)** Representative wide-field images of parental RPE1 *TP53*^{-/-} or *CIP2A*^{-/-} cl#1 cells, stained for DAPI (blue), CIP2A (green) and TOPBP1 (red), in untreated conditions, or after treatment with APH (200 nM, 20 h) or IR (0,25 Gy). **(d)** Quantification of TOPBP1 foci per mitotic cell for data from panel C. The individual values and medians of one experiment are shown. **(e)** Representative wide-field images of RPE1 *TP53* wildtype cells stained for DAPI (blue), CIP2A (green) and TOPBP1 (red), in untreated conditions or after treatment with APH (20 nM, 20 h) or IR (0,25 Gy). **(f)** Quantification of CIP2A and TOPBP1 foci per mitotic cell for data from panel C. Individual values, medians and interquartile range of two biologically independent experiments are shown. **(g)** Representative wide-field images of RPE1 *TP53*^{-/-} cells and two *CIP2A*^{-/-} clones treated with APH (200 nM, 24 h) and stained with DAPI. Arrows indicate micronuclei. **(h)** Quantification of CIP2A foci per mitotic cell in RPE1 *TP53*^{-/-} cells, untreated or treated with APH (200 nM, 20 h), IR (0,25 Gy), ATRi (VE-821, 10 μ M) and/or ATMi (KU55933, 10 μ M). Individual values and medians of two biologically independent experiments are shown. Throughout the figure, 'n' represents the number of cells measured across experiments, and scale bars represents 10 μ m. Source data are provided as a Source data file.

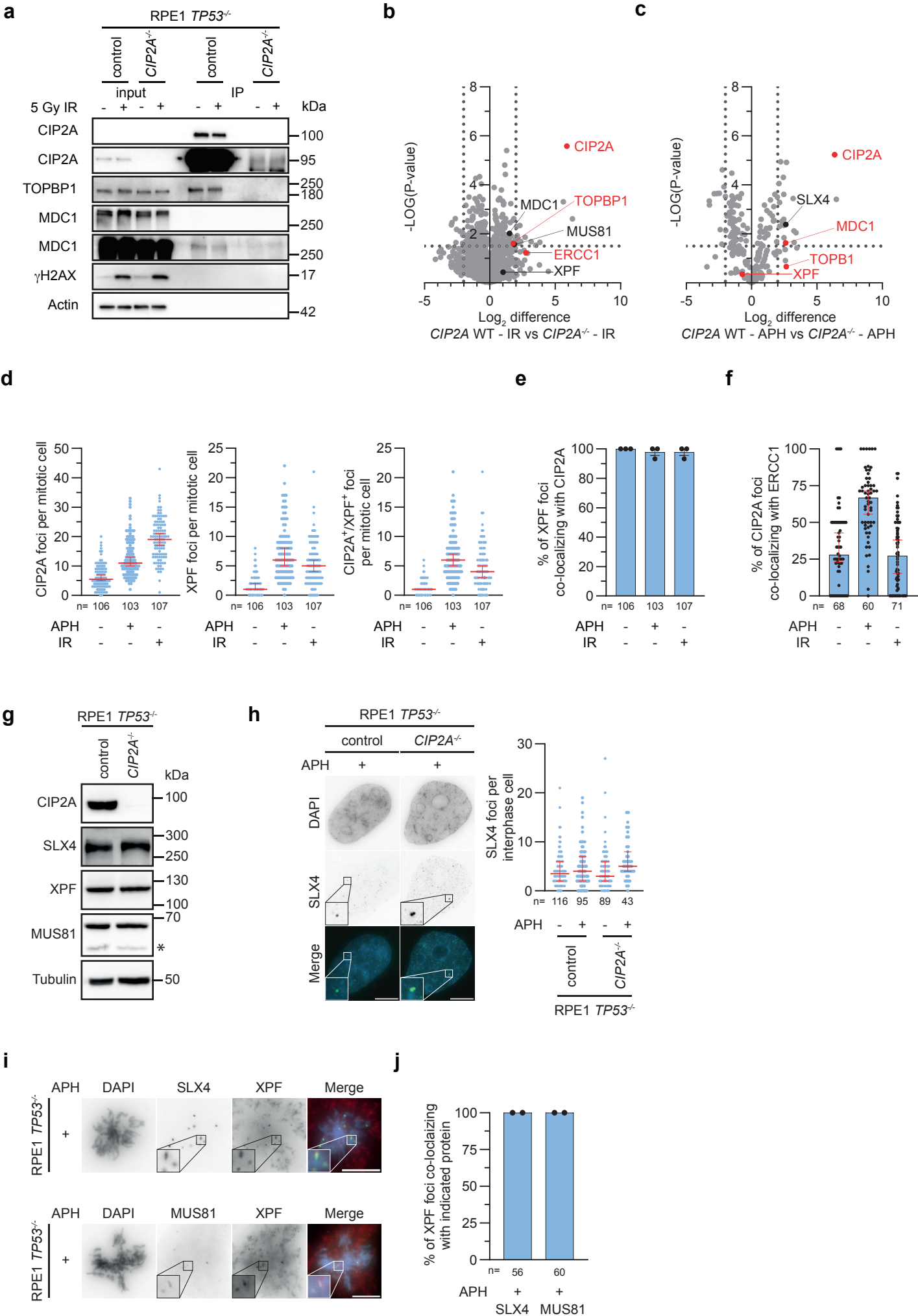
Supplemental Figure 2



Supplemental Figure 2: Overlap between CIP2A-TOPBP1 filamentous complexes and ultrafine bridges

(a) Quantification of CIP2A structures co-localizing with TOPBP1 for data from Figure 1d-e. Bars represent means and SD, and 'n' represents the total number of structures analyzed per treatment, from three biologically independent experiments. **(b)** Quantification of the number of CIP2A foci observed during the different stages of mitosis for RPE1 *TP53*^{-/-} cells treated with APH (200 nM, 20 h). Individual values from two biologically independent experiments are shown. Percentages reflect the number of cells per mitotic phase with at least one CIP2A structure. 'n' represents the total number of cells measured across experiments. **(c)** Representative measurements of the longest axis of STED images of unstructured, loop-containing and filamentous CIP2A-TOPBP1 complexes. For loop-containing structures also the shortest axis is indicated. Arrows indicate the length measurements used in panel D and Fig. 1i for the CIP2A structures shown in Fig. 1d. **(d)** Quantification of the elongation of loop-containing CIP2A-TOPBP1 structures during different stages of mitosis for data from Fig. 1d, e. The dotted line (value: 1) indicates structures with no elongation. Individual values, medians and interquartile range are plotted of three biologically independent experiments. **(E)** RPE1 *TP53*^{-/-} cells treated with APH (200 nM, 20 h). Quantification of the number of PICH⁻ and PICH⁺ indicated CIP2A complexes. Bars represent absolute numbers of CIP2A structures quantified per class from one experiment, from a total of n=124 anaphase cells. Pie graph specifies the number and subtype of the n=71 of PICH⁺ filamentous CIP2A structures (ultrafine bridge, lagging chromosome or chromatin bridge, or PICH foci) from one experiment **(f, g)** Representative Airyscan confocal image of a PICH⁺ CIP2A filamentous structure observed at ultrafine bridges (panel f, scale bar: 4 μ m) or a PICH⁺ CIP2A filamentous structures observed at PICH foci (panel g, scale bars: 2 μ m) for cells as treated as described in panel d. Arrows indicate PICH⁺ UFBs that do not co-localize with CIP2A. For panels a/d/e, 'n' represents the total number of observed structures across experiments. Source data are provided as a Source data file.

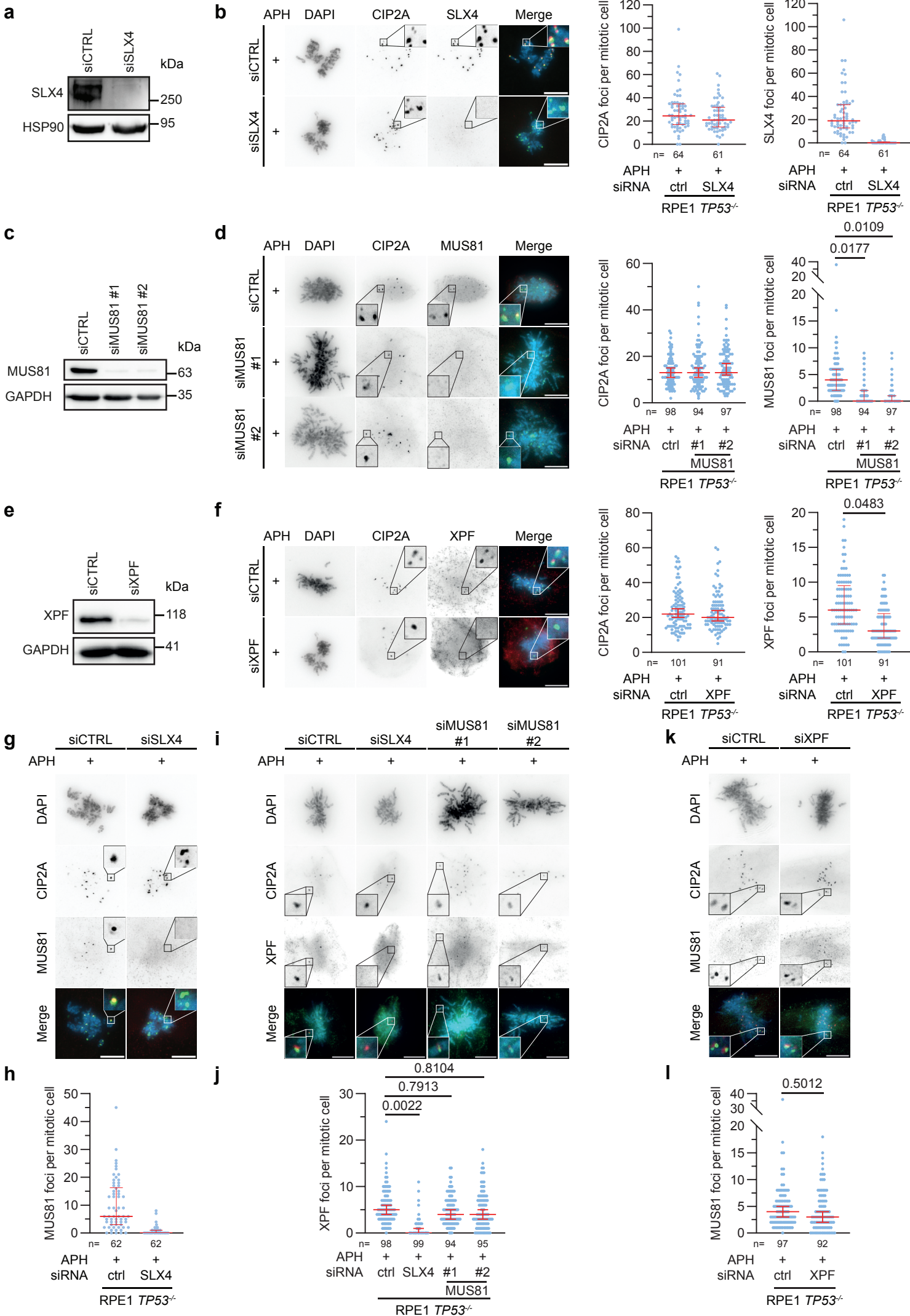
Supplemental Figure 3



Supplemental Figure 3: CIP2A-TOPBP1 mediates mitotic SLX4-ERCC1-XPF-MUS81 recruitment to replication-induced DNA lesions

(a) Western blot analysis of endogenous CIP2A co-immunoprecipitations in mitotic parental RPE1 *TP53*^{-/-} cells and *CIP2A*^{-/-} cl#1 cells after IR (5 Gy). Lysates were immunoblotted for indicated proteins. **(b, c)** Mass spectrometry analysis of mitotic anti-CIP2A immunoprecipitations in untreated parental RPE1 *TP53*^{-/-} versus untreated *CIP2A*^{-/-} cl#1 cells, as controls for MS analysis of IR-treated cells (panel b) or APH-treated cells (panel c). Red: proteins enriched after IR or APH treatment. Black: established CIP2A interactors, or members of the SMX complex that were not enriched after treatment. Two-sided Significance Analysis of Microarrays t-test on three technical replicates. **(d)** Quantification of CIP2A or XPF foci with co-localizing XPF/CIP2A signal per mitotic cell in RPE1 *TP53*^{-/-} cells treated with APH (200 nM, 20 h) or IR (0,25 Gy). Individual values and medians are plotted of three biological independent experiments. **(e)** Quantification of percentage of XPF foci co-localizing with CIP2A per experiment. Medians per experiment are plotted. Bars represent medians and SEM of three biological independent experiments. Two-tailed unpaired t-test was used on medians per experiment. **(f)** Quantification of percentages of CIP2A foci per mitotic cell co-localizing with ERCC1. Bars represent medians and 95% confidence intervals of two biological independent experiments. **(g)** Western blot analysis of parental RPE1 *TP53*^{-/-} cells and *CIP2A*^{-/-} cl#1 cells. Lysates were immunoblotted for indicated proteins. *non-specific band. **(h, i)** RPE1 *TP53*^{-/-} and *CIP2A*^{-/-} cl#1 cells treated with APH (200 nM, 20 h). **(h)** Right: representative wide-field images of cells stained for DAPI (blue) and SLX4 (green). Left: Quantification of interphase SLX4 foci. Individual values, medians and interquartile range of three biologically independent experiments. **(i)** Representative wide-field images of cells stained for DAPI (blue), SLX4 (green), XPF (red) or DAPI (blue), MUS81 (green), XPF (red). **(j)** Quantification of percentages of XPF foci per experiment co-localizing with SLX4 or MUS81 for data from panel i. Bars represent medians of two biologically independent experiments. Throughout the figure, 'n' represents total numbers of cells measured across experiments, and scalebar represents 10 μ m. Source data are provided as a Source data file.

Supplemental Figure 4

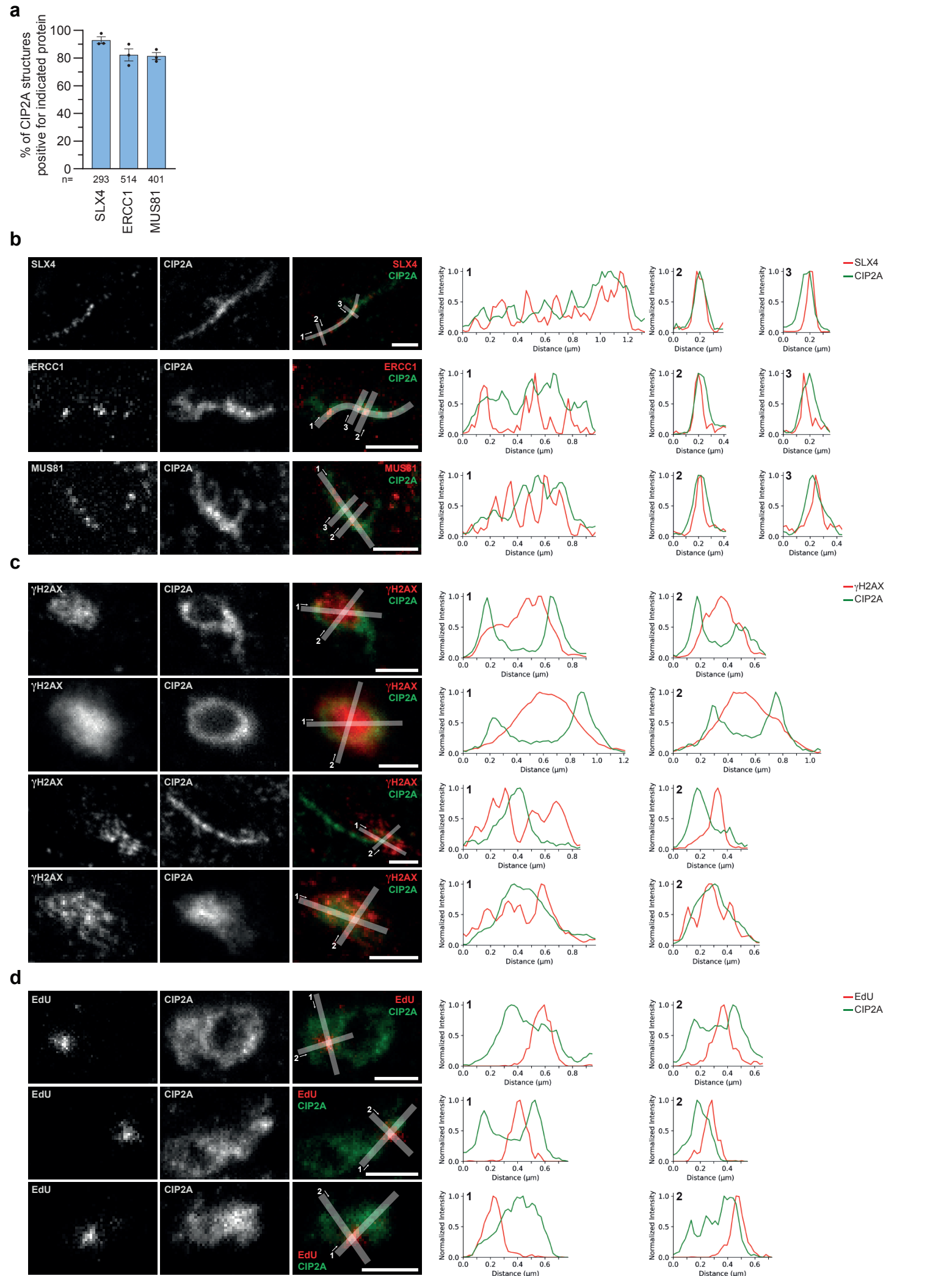


legend on following page

Supplemental Figure 4: CIP2A-TOPBP1 recruit scaffold protein SLX4, to allow further recruitment of entire SMX complex

(a-f) Western blot, imaging and foci quantification of RPE1 *TP53*^{-/-} cells transfected with indicated siRNAs. **(a, c, e)** Lysates were immunoblotted for indicated proteins. **(b, d, f)** RPE1 *TP53*^{-/-} cells were treated with APH (200 nM, 20 h) and transfected with indicated siRNAs. Left: Representative wide-field images of RPE1 *TP53*^{-/-} cells stained for DAPI (blue), CIP2A (green) and SLX4 (red, B), MUS81 (red, panel d) or XPF (red, panel f). Right: quantification of CIP2A and SLX4 (panel b), MUS81 (panel d) or XPF (panel f) per mitotic cell. Individual values, medians and interquartile range of either two (panel b) or three biologically independent experiments (panels d/f) are plotted. Two-tailed unpaired t-test was used on the medians per experiment for panels d/f. **(g-l)** Imaging and quantification of mitotic MUS81 and XPF foci in RPE1 *TP53*^{-/-} cells treated with APH (200 nM, 20 h) and transfected with indicated siRNAs. Representative wide-field images of RPE1 *TP53*^{-/-} cells stained for DAPI (blue), CIP2A (green) and MUS81 (red) transfected with siCTRL or siSLX4 (panel g). Representative wide-field images of RPE1 *TP53*^{-/-} cells stained for DAPI (blue), CIP2A (red) and XPF (green) transfected with indicated siRNAs (i). Representative wide-field images of RPE1 *TP53*^{-/-} cells stained for DAPI (blue), CIP2A (red) and MUS81 (green) transfected with siCTRL or siXPF (k). Quantification of mitotic MUS81 foci (H, L) or mitotic XPF foci (j) for data from panel g, i, k respectively. Individual values, medians and interquartile range of two biologically independent experiments with n>30 cells per experimental condition are plotted. If indicated, a two-tailed unpaired t-test on the medians per experiment was used. Throughout the figure, 'n' represents the total number of cells measured across experiments, and scale bars represent 10 μ m. Source data are provided as a Source data file.

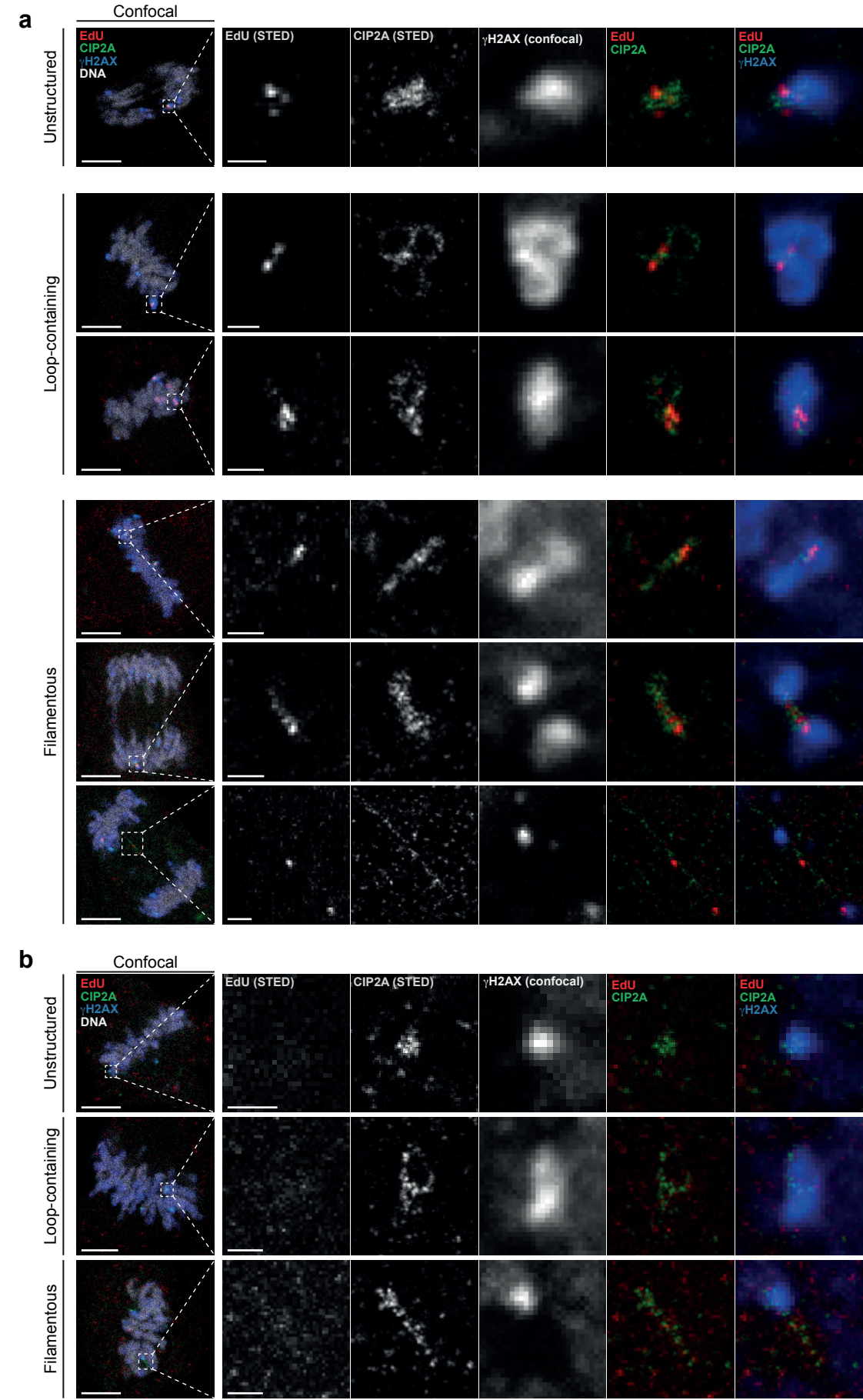
Supplemental Figure 5



Supplemental Figure 5: Line profiles analysis of STED images

(a) Quantification of the percentage mitotic CIP2A structures that co-localized with SLX4, ERCC1 or MUS81 as observed with STED microscopy for RPE1 *TP53*^{-/-} cells as treated in Figure 3. 'n' represents the total number of observed structures measured across three biological independent experiments. **(b)** Line profiles were drawn on dual-color STED images of CIP2A (green) and either SLX4, ERCC1 or MUS81 (red) in panel b, or γH2AX and EdU (red) in panels c, d for RPE1 *TP53*^{-/-} cells, treated as in Figure 3. For each dual-color STED image, 2-3 lines are shown and the corresponding intensity profiles are shown on the right. STED images were processed with only mild background subtraction. Scale bar: 500 nm. Source data are provided as a Source data file.

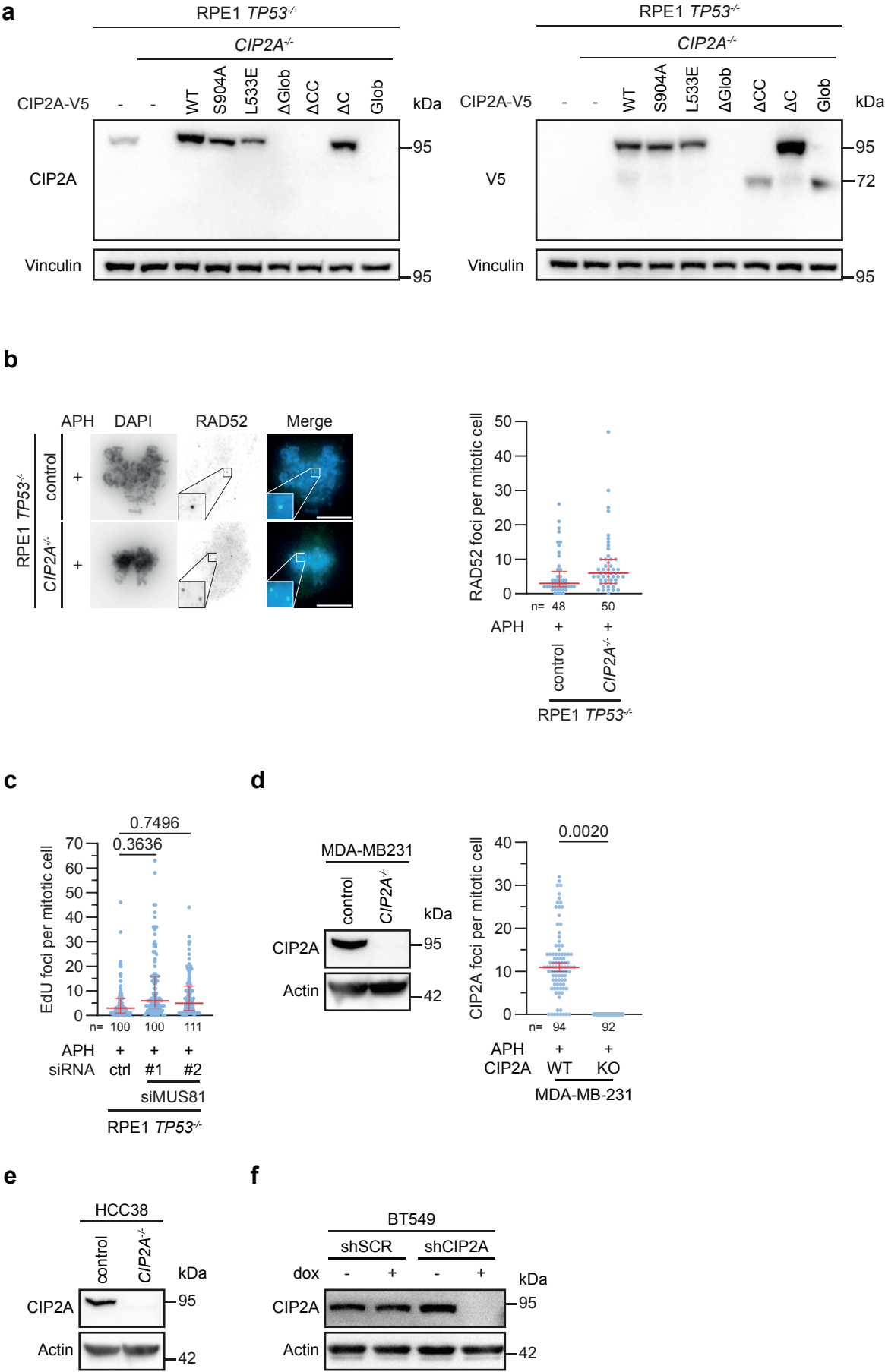
Supplemental Figure 6



Supplemental Figure 6: CIP2A localization in relation to EdU and γ H2AX.

(a, b) RPE1 *TP53*^{-/-} cells were treated with APH (200 nM, 20 h). Representative images of EdU-positive (panel a) and EdU-negative (panel b) unstructured, loop-containing and filamentous CIP2A structures are depicted. Cells were stained for DAPI (white), γ H2AX (blue), CIP2A (green) and EdU (red). Left: confocal overview images. Right: STED images of single CIP2A complexes with superimposed confocal γ H2AX signal. Scale bars: 5 μ m (confocal) or 500 nm (STED).

Supplemental Figure 7

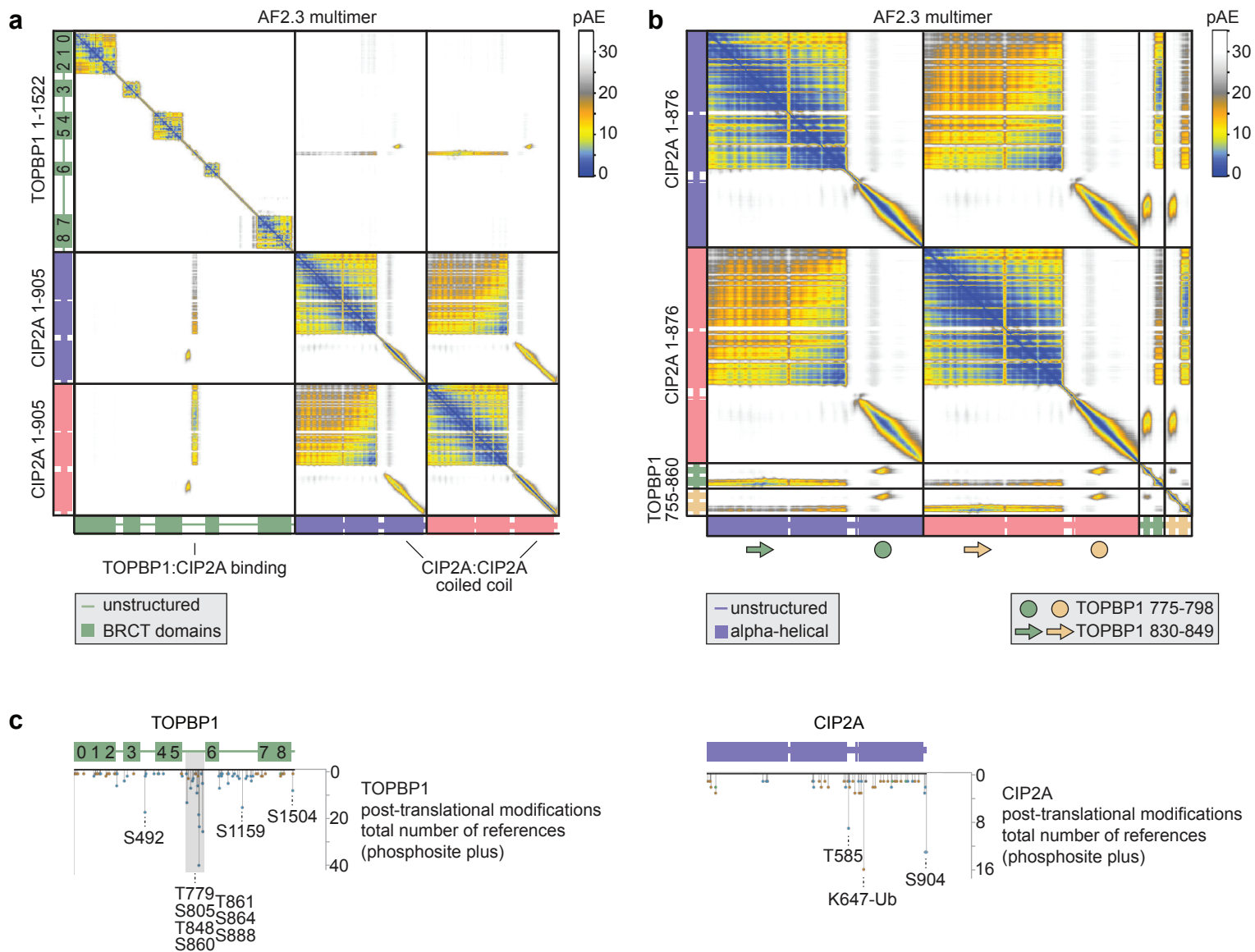


legend on following page

Supplemental Figure 7: CIP2A is not required for MiDAS

(a) Western blot analysis of parental RPE1 *TP53*^{-/-} cells, *CIP2A*^{-/-} cl#1 cells, and *CIP2A*^{-/-} cl#1 cells reconstituted with indicated CIP2A mutants. Lysates were immunoblotted for indicated proteins. **(b)** Right: representative wide-field images of RPE1 *TP53*^{-/-} cells and *CIP2A*^{-/-} cl#1 cells treated with APH (200 nM, 20 h), and stained with DAPI (blue) and RAD52 (green). Scale bar: 10 μ m. Left: quantification of RAD52 foci per mitotic cell for cells as described for right panel. Individual values, medians and interquartile range of one experiment are plotted. **(c)** Quantification of EdU foci per mitotic cell in RPE1 *TP53*^{-/-} cells transfected with indicated siRNAs. Individual values, medians and interquartile range of two experiments are plotted. **(d)** Western blot analysis of CIP2A in parental MDA-MB-231 cells and MDA-MB-231 *CIP2A*^{-/-} cells. Lysates were immunoblotted for indicated proteins. Graph indicates quantification of CIP2A foci per mitotic cell in parental MDA-MB-231 cells and MDA-MB-231 *CIP2A*^{-/-} cells treated with APH (200 nM, 20 h). **(e)** Western blot analysis of CIP2A in parental HCC38 cells and HCC38 *CIP2A*^{-/-} cells. Lysates were immunoblotted for indicated proteins. **(f)** Western blot analysis of CIP2A in untreated or doxycycline-treated BT549 with doxycycline-inducible scramble (shSCR) or CIP2A (shCIP2A) shRNA. Lysates were immunoblotted for indicated proteins. Throughout figure, 'n' represents the total number of cells measured across experiments. Source data are provided as a Source data file.

Supplemental Figure 8

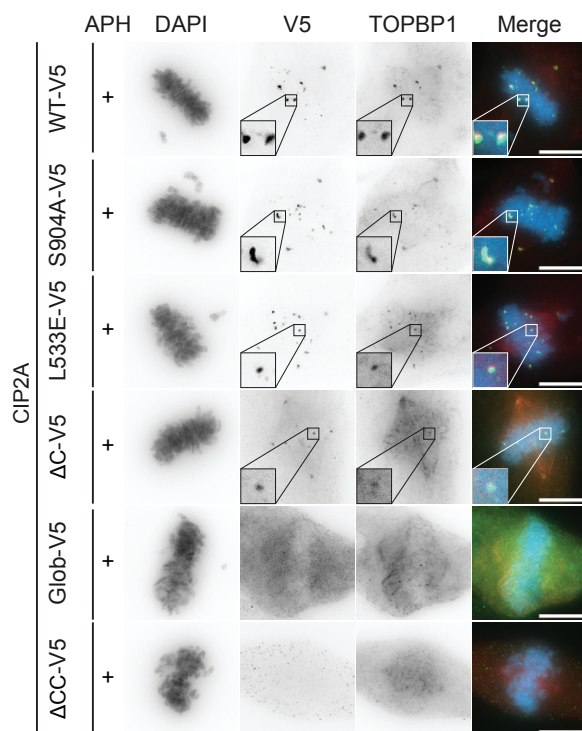


Supplemental Figure 8: Data supporting main figure 5A-C

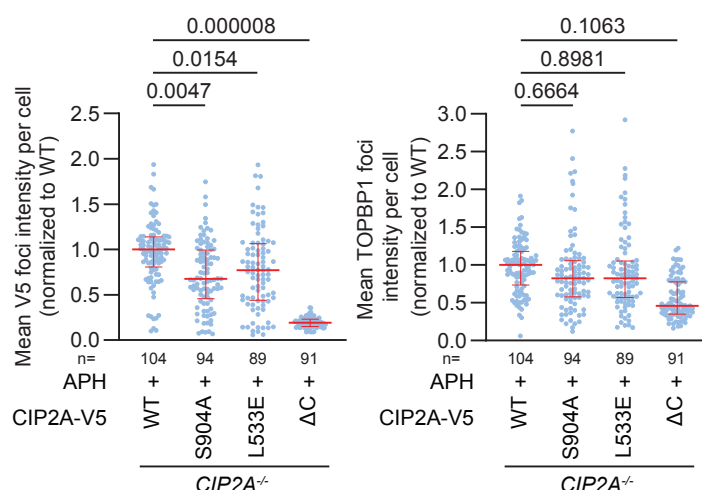
(a, b) Plots with Predicted Aligned Error (PAE) for predictions of (panel a) TOPBP1 1-1522 with 2 copies of CIP2A 1-905 and (panel b) 2 copies of CIP2A 1-876 with 2 copies of TOPBP1 755-860. Low pAE scores indicated proximities with high confidence. Structural features apparent from this analysis include i) an extensive and high confidence CIP2A:CIP2A coiled coil interaction interface mediated by CIP2A's C-terminal region, ii) the putative interaction of TOPBP1 755-798 to the CIP2A coiled coil, and iii) the putative interaction of TOPBP1 830-849 with the globular N-terminal region of CIP2A. **(c)** Mapping of post-translational modification (phosphosite plus) on the sequences of TOPBP1 and CIP2A. Modifications detected in 8 or more studies are indicated.

Supplemental Figure 9

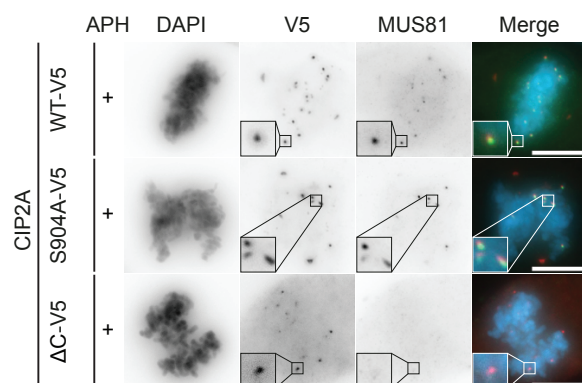
a



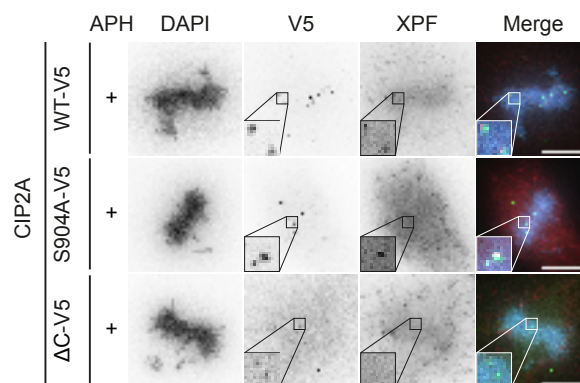
b



c



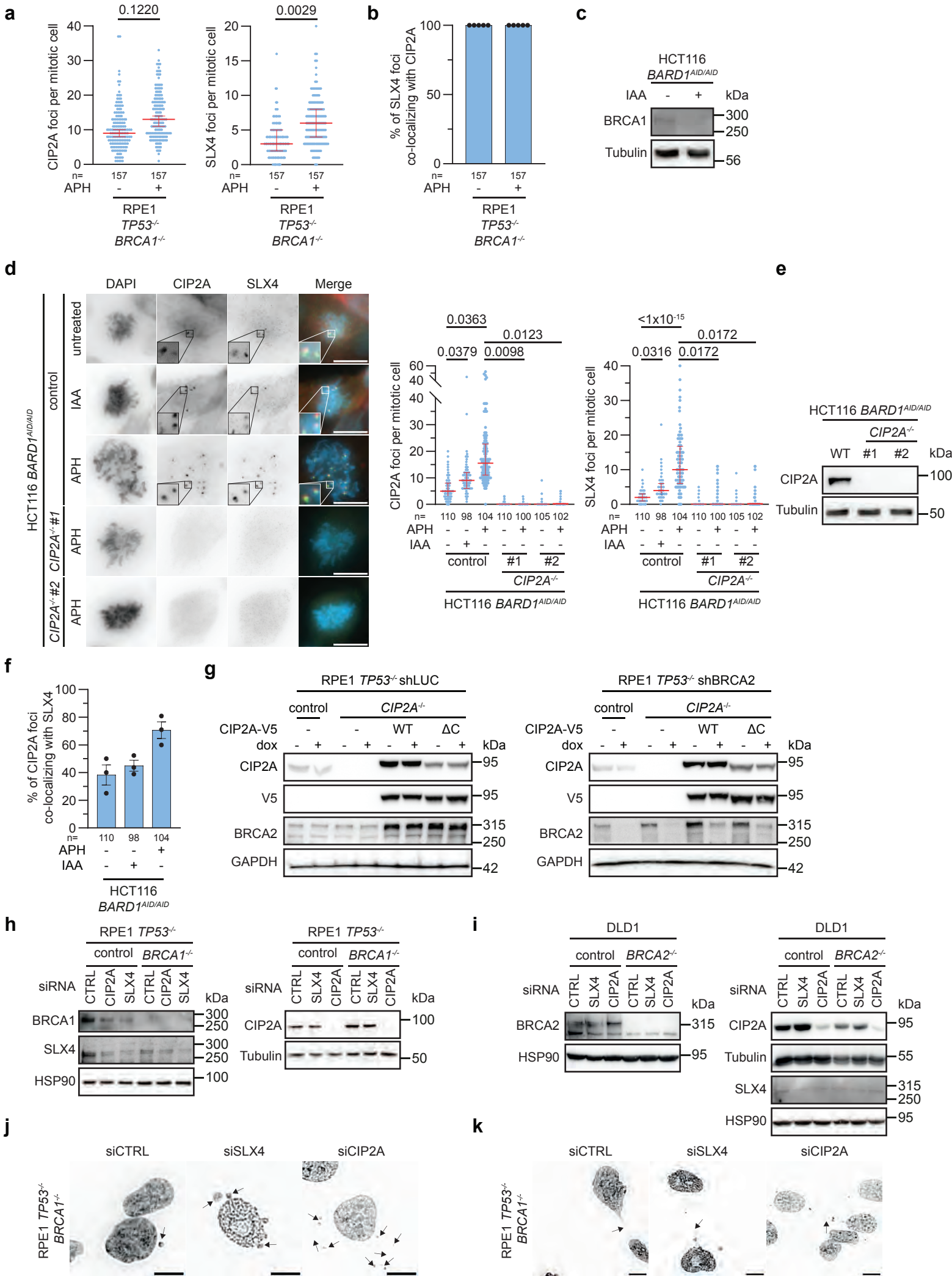
d



Supplement Figure 9: C-terminal domain of CIP2A is required for functional CIP2A-TOPBP1 complex and MUS81 recruitment

(a) Representative images of *CIP2A*^{-/-} cl#1 reconstituted with indicated CIP2A mutants stained for DAPI (blue), V5 (green) and TOPBP1 (red) treated with APH (200 nM, 20 h). **(b)** Quantification of mean V5 foci and mean TOPBP1 foci intensity per mitotic cell for data from panel a, normalized to median foci intensity of *CIP2A*^{-/-} cells reconstituted with CIP2A-WT. Individual values, medians and interquartile range of three biologically independent experiments are plotted. 'n' represents the total number of cells measured across experiments. Ordinary one-way ANOVA with Dunnett's multiple comparison test was used on the medians per experiment. **(c)** Representative images of *CIP2A*^{-/-} cl#1 reconstituted with either CIP2A-WT, CIP2A-S904A or CIP2A-ΔC stained for DAPI (blue), V5 (red) and MUS81 (green) treated with APH (200 nM, 20 h). **(d)** Representative images of *CIP2A*^{-/-} cl#1 reconstituted with either CIP2A-WT, CIP2A-S904A or CIP2A-ΔC stained for DAPI (blue), V5 (green) and XPF (red) treated with APH (200 nM, 20 h). Throughout the figure, scale bars represent 10 μm. Source data are provided as a Source data file.

Supplemental Figure 10



Supplemental Figure 10: Consequences of CIP2A or SLX4 loss in BRCA1, BRCA2, or BARD1 defective cells.

(a, b) RPE1 *TP53*^{-/-} *PAC*^{-/-} *BRCA1*^{-/-} cells were treated with APH (200 nM, 20 h). Panel a: Quantification of CIP2A and SLX4 foci per mitotic cell. Individual values, medians and interquartile range of five biologically independent experiments are plotted. Panel b: Quantification of percentage of SLX4 foci co-localizing with CIP2A foci. Median values per experiment are plotted. Bars represent the mean of five biologically independent experiments. For panels a and b, two-tailed unpaired t-tests were used on medians per experiment. **(c)** Western blot analysis of HCT116 *BARD1*^{AID/AID} cells treated with auxin (IAA, 1 mM, 24 h). Lysates were immunoblotted for indicated proteins. **(d)** Left: representative wide-field images of parental HCT116 *BARD1*^{AID/AID} or *CIP2A*^{-/-} clones, stained for DAPI (blue), CIP2A (red), SLX4 (green). Left: Untreated, treated with APH (200 nM, 20 h) or IAA (1 mM, 72 h). Right: Quantification of CIP2A and SLX4 foci per mitotic cell. Individual values, medians and interquartile range of three biologically independent experiments are plotted. Two-tailed unpaired t-test was used on medians per experiment. **(e)** Western blot analysis of parental HCT116 *BARD1*^{AID/AID} or *CIP2A*^{-/-} clones for indicated proteins. **(f)** Quantification of percentage of CIP2A foci co-localizing with SLX4, for data from panel e. Median values per experiment are plotted. Bars represent means and SEM of three biologically independent experiments. **(g)** Western blot analysis for indicated proteins of doxycycline-treated RPE1 *TP53*^{-/-} cells, *CIP2A*^{-/-} cl#1 cells and *CIP2A*^{-/-} cl#1 cells reconstituted with indicated CIP2A mutants, with doxycycline-inducible shLUC or shBRCA2. **(h, i)** Western blot analysis for indicated proteins of RPE1 *TP53*^{-/-} *PAC*^{-/-} and RPE1 *TP53*^{-/-} *PAC*^{-/-} *BRCA1*^{-/-} cells (h) or DLD1 WT and DLD1 *BRCA2*^{-/-} cells (i) transfected with indicated siRNAs. **(j, k)** Representative wide-field images of RPE1 *TP53*^{-/-} *PAC*^{-/-} *BRCA1*^{-/-} cells transfected with indicated siRNAs and stained for DAPI. Arrows indicate either micronuclei (panel j), or nucleoplasmic bridges (panel k). Throughout the figure, 'n' represents the total number of cells measured across experiments, and scale bar represents 10 μ m. Source data are provided as a Source data file.